Journal of Hazardous Materials 174 (2010) 368–374

Contents lists available at ScienceDirect

Journal of Hazardous Materials

journal homepage: www.elsevier.com/locate/jhazmat

Photodegradation of chloroform in aqueous solution: Impact of montmorillonite KSF particles

Jing Li[a,b], Feng Wu[a,**], Gilles Mailhot[b,c,*], Nansheng Deng[a]

[a] Department of Environmental Science, School of Resources and Environmental Science, Wuhan University, Wuhan, 430079, China
[b] Clermont Université, Université Blaise Pascal, Laboratoire de Photochimie Moléculaire et Macromoléculaire, BP 10448, F-63000, Clermont-Ferrand, France
[c] CNRS, UMR 6505, Laboratoire de Photochimie Moléculaire et Macromoléculaire, F-63177, Aubière, France

ARTICLE INFO

Article history:
Received 10 June 2009
Received in revised form
11 September 2009
Accepted 11 September 2009
Available online 19 September 2009

Keywords:
Chloroform
Montmorillonite KSF
Photodegradation
Carboxylic salts

ABSTRACT

In this work, photodegradation of chloroform in water suspensions of montmorillonite KSF (KSF) under a black light lamp (λ = 365 nm) was investigated. The results showed that KSF induced the photodegradation of chloroform by producing hydroxyl radical (•OH) that oxidized chloroform in the heterogeneous clay–water systems. The photodegradation of chloroform in KSF suspensions was greatly influenced by the concentration of KSF and the pH of KSF suspensions. The photodegradation of chloroform by KSF followed the Langmuir–Hinshelwood Model. Furthermore, the removal efficiency of chloroform can be enhanced by the presence of carboxylates (oxalate and citrate) and humic acid (HA). This work demonstrates that KSF can be used as a new and efficient photocatalyst in oxidation and removal of organic compounds.

1. Introduction

Chloroform has been used in a wide range of industrial processes and to produce industrial products, for example, lubricants, cleaning solvents, paper bleaching, and intermediates for pharmaceuticals, herbicides and fungicides. Unfortunately, emissions of this compound are harmful to the environment, and in particular it is an important contributor to the destruction of the ozone layer [1]. It is important to find reliable methods to convert it to less harmful compounds. One promising method of destroying a wide spectrum of organic compounds is photocatalytic degradation. Heterogeneous photocatalysis process has gained significant impetus over the last few years to treat different media containing various types of pollutants [2,3].

Among heterogeneous photocatalytic systems, clay photochemical systems have received particular attention recently. Research of clay photochemical detoxification has mainly focused on two types, namely the clay–photo-Fenton system (Fe-clay/H_2O_2/UV) and clay photocatalytic system. Much attention has been paid to the clay–photo-Fenton reaction and the modified clay photocatalysis due to their high photocatalytic activity as well as their prospective application to wastewater detoxification [4–7]. As far as we know, there are few studies concerning raw clay photocatalysis [8]. In any case, new clay photocatalysts are constantly in great demand.

Montmorillonite, a representative natural clay mineral, possesses a layered structure: two silica tetrahedral sheets and an alumina octahedral sheet. It has the capacity of adsorbing a multitude of organic and inorganic compounds which is favorable for the photocatalysis reaction [9,10]. Montmorillonite contains metal impurities resulting from isomorphous substitution, for instance, Al^{3+} or Fe^{3+} substitution for Si^{4+}, and Fe^{2+}, Mg^{2+} or Zn^{2+} substitution for Al^{3+}. It has been suggested that iron cations in the clay are responsible for the generation of reactive oxygen radicals according to the well-known Haber–Weiss cycle [11].

Montmorillonite KSF (KSF) has been widely used as a catalyst for organic synthesis and as an ion-exchange material in the removal of heavy metals from standard solutions [12,13]. In this paper, its photocatalytic ability for chloroform degradation in a heterogeneous system was investigated using commercially available KSF. The main influencing factors, such as suspension pH, the concentrations of KSF and chloroform, presence of carboxylic acids (oxalate and citrate), or humic acid (HA) were examined. This work implies that KSF is a potential photocatalyst for removal of chloroform from wastewater.

* Corresponding author at: Clermont Université, Université Blaise Pascal, Laboratoire de Photochimie Moléculaire et Macromoléculaire, F-63000, Clermont-Ferrand, France. Tel.: +33 0 4 73 40 71 73; fax: +33 0 4 73 40 71 73.
** Corresponding author. Tel.: +86 27 68778511; fax: +86 27 68778511.
E-mail addresses: fengwu@whu.edu.cn (F. Wu), gilles.mailhot@univ-bpclermont.fr (G. Mailhot).

0304-3894/$ – see front matter © 2009 Elsevier B.V. All rights reserved.
doi:10.1016/j.jhazmat.2009.09.061

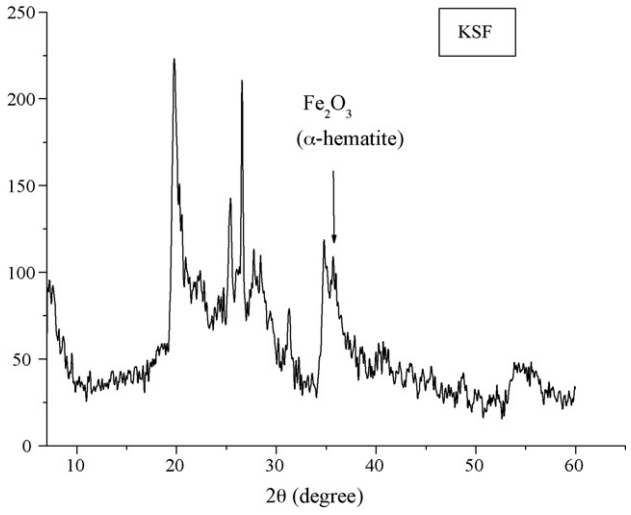

Fig. 1. Powder XRD pattern of the montmorillonite KSF.

2. Experimental

2.1. Chemicals

Chloroform was purchased from Fisher Scientific (Santa Clara, CA). HA was obtained from Aldrich Chemical Company, Inc. (Milwaukee, WI, USA) and used without further purification. Sodium oxalate and sodium citrate (Sigma–Aldrich) were used as carboxylic acid. Hydrochloric acid (HCl) and sodium hydroxide (NaOH) were used to adjust the pH values of the solutions. All the other reagents were of analytical grade. Water was treated with an ultrapure water system (Liyuan Electric Instrument Co., Beijing, PRC) and purified water with 18 MΩ cm resistivity was used throughout this work.

2.2. Minerals

Montmorillonite KSF was purchased from Alfa Aesar (A Johnson Matthey Company, Ward Hill, MA, USA). The surface area of KSF was 46 $m^2\ g^{-1}$ (N_2-BET method). KSF is an acid-treated bentonite and the acid treatment destroys the structure of raw montmorillonite. The XRD pattern of KSF is shown in Fig. 1. The specific diffraction peak at $2\theta = 35.6^\circ$ is assigned to the Fe_2O_3 (α-hematite) crystallite. The chemical compositions of KSF were determined by XRF (Table 1).

2.3. Photochemical experiment

The experiments were conducted in 22 mL headspace vials with screwtop cap and Teflon-faced septum. The light source was GHF 125 Black light high pressure mercury lamp (125 W, Xinghui Special Lamps Co., Changsha, China) with emission light at wavelength of 365 nm (band width less than 10 nm). The intensity of irradiation at 10 cm distance was about 1.5 mW/cm^2. The volume of each suspension was 10 mL. All suspensions containing exact amounts of chloroform and KSF were prepared and mixed completely. The suspension pH was adjusted using dilute HCl or NaOH. After all the chemicals were transferred to the vials, the vials were immediately capped tightly with the Teflon-faced septum. The vials were placed on a rotary shaker to maintain the uniformity of the suspensions, and photolyzed under a black light lamp at a distance of 10 cm for a period of 10 h. The temperature of the irradiated vials was maintained at 25 ± 1 °C by an air-cooled temperature control system. At different time intervals (2 h), one headspace vial was taken out for sampling and analysis. Control experiments at different pH values were carried out under identical conditions, but in the dark. Every experiment was performed in triplicate and the obtained errors are less than 5%.

Table 1
Chemical compositions of KSF.

Component	%
Na_2O	0.0573
MgO	4.31
Al_2O_3	16.3
SiO_2	49.1
SO_3	22.3
K_2O	0.495
CaO	2.30
TiO_2	0.210
MnO	0.0191
Fe_2O_3	4.76
Ignition loss	0.149

2.4. Analysis

Solid-phase microextraction (SPME) with subsequent GC determination was used for the analysis of chloroform. SPME devices were obtained from Supelco (Bellefonte, PA, USA) and equipped with 100 μm polydimethylsiloxane (PDMS) coating fiber. A Shimadzu 14C GC equipped with FID detector using nitrogen as the carrier gas, a split/splitless injector operating in split mode and a capillary column (SPB-5, 30 m × 0.32 mm × 0.25 μm) were used. Operating conditions were as follows: detector temperature 240 °C, injector temperature 220 °C, column temperature 60 °C, split ratio 10:1, carrier gas flow-rate 1.5 mL min^{-1}, air/H_2 ratio 10:1.

At different time intervals (2 h), the illuminated sample vials were taken out and placed in a digital circulating water bath at 45 °C for 30 min. Then the fiber was introduced through the septum and kept in the headspace of the vial for 5 min at 45 °C. Subsequently the fiber was withdrawn into the SPME syringe needle, which was then pulled out of the sample vial and immediately inserted into the GC injection port for desorption. Desorption was conducted at 220 °C for 1.5 min. Finally the target compounds were analyzed under the chromatographic conditions described above. For detection of intermediates and final products, a GC–MS (Agilent 6890 series, using a HP-5.5% phenyl methyl siloxane column (30.0 m × 0.32 mm × 0.25 μm), and mass selective detector MSD 5973) was used and gaseous samples were manually injected into the GC using a 100 mL gas-tight syringe.

After SPME-GC or GC–MS analysis, the aqueous phase in the sampling vial was analyzed by ionic chromatography (IC) for chloride ions. The IC system was a Dionex Bio-LC system equipped with a conductivity detector and a Dionex OmniPac PAX-500 column (250 mm × 5 mm × 8 μm). A mixture of 1 mM Na_2CO_3 and 0.1 mM $NaHCO_3$ solution was used as eluent at a flow-rate of 1 mL min^{-1}. A sample (10 mL) of supernatant was filtered with a 0.22 μm membrane filter, and injected into the column through a 10 μL sample loop.

The concentrations of iron ions in the clay suspensions at different initial pH values were determined by using *ortho*-phenanthroline as a complexing agent of Fe^{2+}. The measured wavelength of 510 nm used to determine the Fe^{2+} concentration was the maximum for the complex between *ortho*-phenanthroline and Fe^{2+} [14]. The KSF suspension supernatants were separated by centrifugation and used for determination of Fe^{2+}. Fe^{3+} ions in the supernatants were reduced to Fe^{2+} with excess ascorbic acid and the total concentrations of iron ions were determined in terms of Fe^{2+}. Fe^{3+} concentrations were calculated by subtracting Fe^{2+} concentrations from the total concentrations of iron ions.

The amount of $^{\bullet}OH$ radicals produced in KSF suspensions was determined according to the method reported by Liu et al. [15]. Ben-

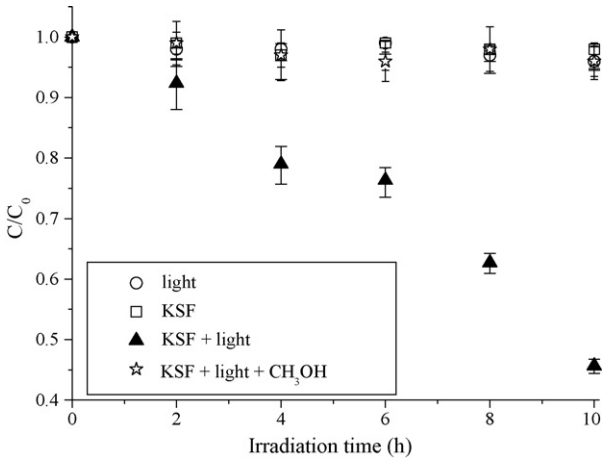

Fig. 2. Kinetics of chloroform degradation as a function of irradiation time in different conditions. The experimental conditions were as follows: initial concentration of chloroform 0.42 mM, KSF 2.0 g L^{-1}, irradiation time 10 h, pH 3.8, initial concentration of CH_3OH 433 mM.

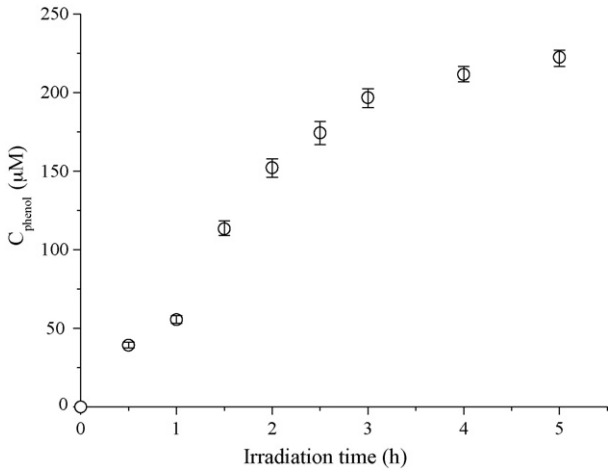

Fig. 3. Formation of phenol (hydroxyl radicals) in the KSF suspensions. Benzene was used as a scavenger of •OH radicals. The experimental conditions were as follows: KSF 2 g L^{-1}, Benzene 7 mM, pH 3.8, irradiation time 5 h.

zene was used as the probe. It was regarded that the •OH oxidation of benzene forms phenol with 100% yield and the phenol concentration represented the concentration of hydroxyl radicals [15]. 7 mM benzene was added to the KSF suspensions. Phenol concentration was detected by HPLC. The detection wavelength was 280 nm and the mobile phase was the mixture of methanol/water (70/30, v/v) at a flow-rate of 1.0 mL min^{-1}.

The X-ray diffraction (XRD) patterns were recorded on a Dmax-rA diffractometer (Rigaku, Japan) using a Cu Kα as X-radiation source, operated at 40 kV and 30 mA.

3. Results and discussion

3.1. Photoinduced degradation of chloroform in KSF suspensions

As shown in Fig. 2, in the absence of KSF the degradation of chloroform under UV irradiation is negligible. This indicates that chloroform cannot be degraded by direct photolysis under irradiation at 365 nm [16]. In the presence of KSF, the degradation of chloroform in the dark control up to 10 h was negligible, while the photodegradation efficiency of chloroform was 54% after 10 h of irradiation. Thus KSF induced the photodegradation of chloroform. However, no photodegradation of chloroform was found in irradiated solutions when 433 mM of methanol was added into the KSF suspension. Since methanol at high concentrations played the role of scavenger for •OH radical, it significantly inhibited the degradation of chloroform. This result indicated that •OH might be involved in the degradation of chloroform in the KSF irradiation system.

The hydroxyl radical is a nonspecific oxidant that can effectively degrade most organic pollutants. The formation of •OH under UV irradiation was detected in the suspension containing 2 g L^{-1} KSF and 7 mM of benzene at pH 3.8. As shown in Fig. 3, the concentration of •OH (phenol) increased with the irradiation time and more than 0.2 mM •OH (phenol) were produced after 5 h of irradiation.

Because of the low chloroform concentration and the fact that most of the possible intermediaries have a short-life time as reported [17], the distinguishable products were simply carbon dioxide and chloride ion in this work. This was consistent with the work of Kormann et al. [18] and Choi and Hoffmann [19], who studied chloroform photooxidation by •OH in aqueous TiO_2 suspensions in the presence of dissolved oxygen. It is supposed that firstly $CHCl_3$ is degraded by •OH (Eq. (1)) via the H abstraction and then $•CCl_3$ further reacts with dissolved oxygen in the solution, •OH, HO_2• and H_2O to produce Cl^- and CO_2 (Eq. (2)).

$$CHCl_3 + •OH \rightarrow •CCl_3 + H_2O \quad (1)$$

$$•CCl_3 \xrightarrow{O_2, OH, H_2O} \cdots \rightarrow Cl^- + CO_2 \quad (2)$$

The mechanism in the presence of oxygen can be detailed with the following equations (Eqs. (3)–(6)):

$$•CCl_3 + O_2 \rightarrow •OOCCl_3 \quad (3)$$

$$2•OOCCl_3 \rightarrow 2•OCCl_3 + O_2 \quad (4)$$

$$•OCCl_3 \rightarrow Cl_2C{=}O + Cl• \quad (5)$$

$$Cl_2C{=}O + H_2O \rightarrow CO_2 + 2H^+ + 2Cl^- \quad (6)$$

3.2. Effect of clay concentration

The effect of clay (KSF) concentration on the photodegradation of chloroform was studied in the range from 0 to 10.0 g L^{-1} at pH 3.8. As shown in Fig. 4, the photodegradation efficiency of chloroform increased when the concentration of clay in aqueous solutions was increased in the range from 0 to 4.0 g L^{-1}. At higher concentrations such as 6.0 and 10.0 g L^{-1} of clays, the photodegradation efficiency of the chloroform was strongly reduced. Thus an appropriate clay

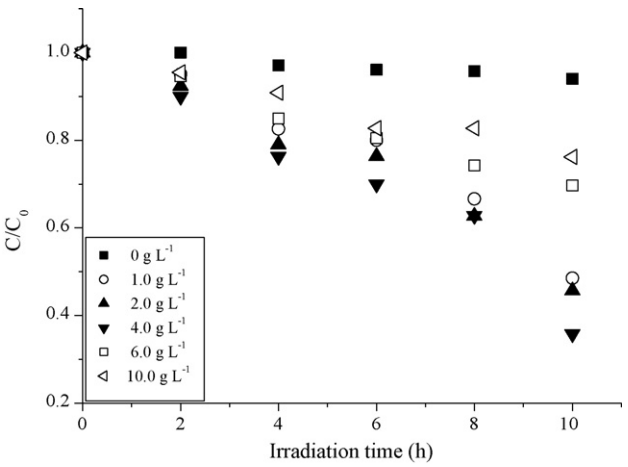

Fig. 4. Influence of clay concentration on the photodegradation of chloroform in aqueous solutions containing KSF at different concentrations in the range of 0–0.0 g L^{-1}. The experimental conditions were as follows: chloroform 0.42 mM, irradiation time 10 h, pH 3.8.

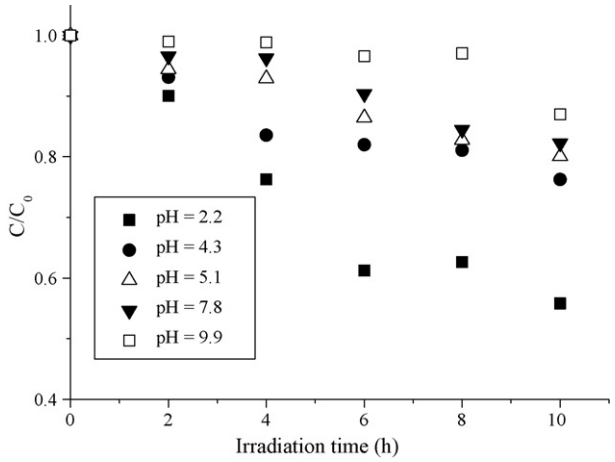

Fig. 5. Influence of pH on the photodegradation of chloroform in aqueous solutions containing KSF at various pH values. The experimental conditions were as follows: KSF 2.0 g L^{-1}, chloroform 0.42 mM, irradiation time 10 h.

concentration facilitates the degradation of chloroform in clay suspensions. However, when the clay concentration was raised to a threshold value, the suspended clay particles considerably weakened light penetration into the suspensions due to a shielding effect [3,20]. Consequently the degradation rate of chloroform decreased. In our experimental conditions, the optimal concentration of KSF was around 4.0 g L^{-1}.

3.3. Effect of initial pH

Montmorillonite KSF is acid-activated clay containing relatively high amount of iron. Variation of the initial pH value of the clay suspension changes the clay particle properties such as surface charge, surface area and surface hydroxyl group [21] and the amount of photoactive iron species dissolved from the clay into the solutions. To observe the effect of pH on the photodegradation of chloroform, five experiments were conducted with the same initial chloroform concentration of 0.42 mM, KSF concentration of 2 g L^{-1} but at different pH values (2.2, 4.3, 5.1, 7.8, and 9.9). As shown in Fig. 5, the results show that the chloroform degradation rate is strongly pH-dependent. The chloroform degradation rate increased when the pH of KSF suspensions was reduced within the range of 9.9–2.2, increasing in particular by 1.5 times between pH 4.3 and 2.2, but only slightly in the higher pH solutions, i.e. between 4.3 and 9.9. KSF contains 4.76% of the iron component that is composed of free iron oxides that distribute randomly on the clay surface, and structural iron in the octahedral lattice [22]. We detected the amount of free iron ions, including Fe^{2+} and Fe^{3+}, dissolved in the suspensions (Table 2) at different pH values. The total amount of free iron ions was increased by acidifying the suspensions from pH 5.1 to 2.2. The ferric ion species, especially $Fe(OH)^{2+}$, are the most important photochemical sources of hydroxyl radical and are more abundant at acid pH in the region of 3.0 [23], which could lead to the formation of •OH via reaction Eq. (7). Therefore, the variation of degradation efficiency of chloroform at acid pH values was mainly attributed to the pH dependence of the amount of iron ions and their speciation. But at higher pH than 5, there is almost no soluble iron in the suspended solutions, so the chloroform photodegradation could be attributed to the reactions at the clay surface. Anyway, the results shows that this process is negligible compared to the •OH radical reaction. The pH effect reflects that iron present in the clay is the most important photochemical source of •OH radicals which induce the photodegradation of chloroform.

Table 2
Amount of iron ions dissolved in clay suspensions.

	Concentration of iron ions (μM)					
	pH 2.2		pH 4.3		pH 5.1	
KSF suspension (2 g L^{-1})	Fe^{3+} 93.38	Fe^{2+} 77.30	Fe^{3+} 9.64	Fe^{2+} 56.30	Fe^{3+} 0.38	Fe^{2+} 32.48

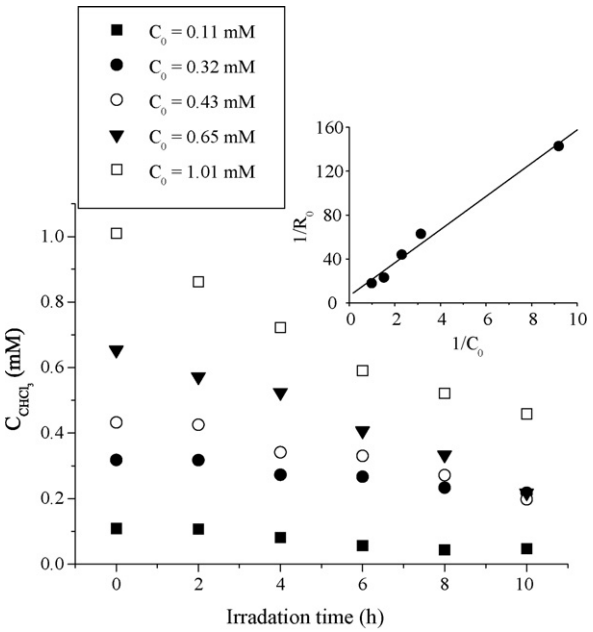

Fig. 6. Influence of the initial concentration of chloroform on chloroform photodegradation in the KSF suspensions. *Inset*: plots of $1/R_0$ versus $1/C_0$. The experimental conditions were as follows: initial concentration of chloroform: 0.11, 0.32, 0.43, 0.65, and 1.01 mM, KSF 2.0 g L^{-1}, irradiation time 10 h, pH 3.8.

$$Fe(OH)^{2+} \xrightarrow{h\upsilon} Fe^{2+} + {}^{\bullet}OH \quad (7)$$

3.4. Effect of initial concentration of chloroforms

Under the conditions of 2 g L^{-1} KSF and at pH 3.8, the effect on photodegradation of the initial chloroform concentration in the range of 0.11–1.01 mM was analyzed. Fig. 6 shows the concentration profile variation of chloroform at different initial concentrations in KSF suspended solutions. The initial rates of the reaction were determined by extrapolating the tangent (based on the linear fit of the first four points) of the concentration profile back to initial conditions. The slopes calculated at the initial three to five points were almost identical, indicating the accuracy of the initial rates obtained in this study. It is proposed that the degradation kinetics of chloroform could be described according to the Langmuir–Hinshelwood rate law (L–H equation) as follows (Eq. (8)):

$$R_0 = -\frac{dC}{dt} = \frac{kKC_0}{1 + KC_0} \quad (8)$$

where C_0 is the initial concentration and k, K are rate constant and the adsorption coefficient respectively. The linear form of L–H equation (Eq. (9)) is

$$\frac{1}{R_0} = \frac{1}{kK}\frac{1}{C_0} + \frac{1}{k} \quad (9)$$

Thus, a plot of $1/R_0$ versus $1/C_0$ should give a straight line. As shown in the inset of Fig. 6, there was a good linear relationship between $1/R_0$ and $1/C_0$. Through the linear fit of the curve in the

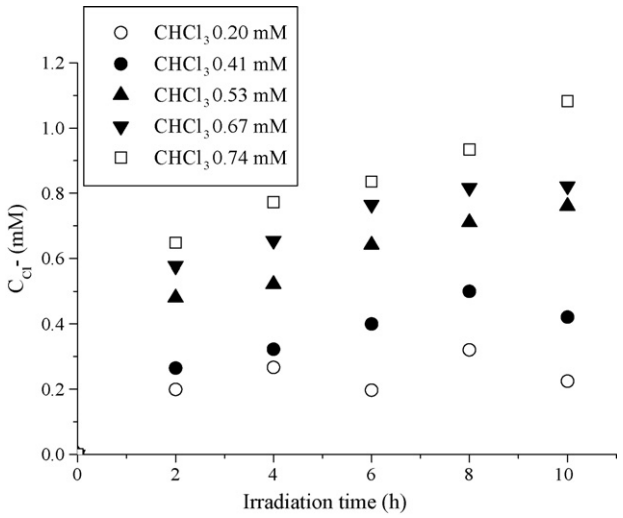

Fig. 7. Release of chloride ion during the photodegradation of chloroform. The experimental conditions were as follows: initial concentration of chloroform: 0.20, 0.41, 0.53, 0.67, and 0.74 mM, KSF 2.0 g L^{-1}, irradiation time 10 h, pH 3.8.

inset in Fig. 6, we obtained the equation (Eq. (10)):

$$\frac{1}{R_0} = 15.12 \times \frac{1}{C_0} + 6.24 \quad (R = 0.9927) \tag{10}$$

So the value of rate constant k and the adsorption coefficient K was calculated to be 0.16 mM h^{-1} and 0.41 mM^{-1} respectively. Thus in the KSF suspension the kinetic equations of the photodegradation of chloroform can be expressed as (Eq. (11)):

$$R_0 = \frac{0.066C_0}{1 + 0.41C_0} \tag{11}$$

In order to observe the release of chloride ions in chloroform photodegradation, experiments with another series of different initial concentrations of chloroform were conducted. Fig. 7 shows stoichiometric release of chloride ions with chloroform loss at each sampling time. The mass balance between the amount of the chloride ion produced and that of the decreased chloroform was in good accordance with the experimental results. The stoichiometric ratio of $[Cl^-]_{production}/[CHCl_3]_{degraded}$ was 2.10 ± 0.11, which may be due to the different ways of $^{\bullet}CCl_3$ reaction giving rise not only to Cl^- but also other chlorinated compounds. This is consistent with the results of Calza et al. [24], who observed a similar ratio of $[Cl^-]_{production}/[CHCl_3]_{degraded}$ in experiments using TiO_2 as photocatalyst in the presence of oxygen.

3.5. Effect of carboxylic anions

Carboxylic acids are widespread organic compounds in aquatic environment and could form strong ligand-to-metal charge absorption bands with iron in the near-UV and visible region [23]. So it is interesting to investigate the effect of carboxylic anions on the degradation of chloroform in KSF suspensions. The degradation efficiency of chloroform in the irradiated system containing different initial citrate or oxalate concentrations was tested. It was found that the chloroform degradation rate could be enhanced in a limitative range of carboxylic salt concentrations. As shown in Fig. 8, the removal efficiency of chloroform increased in the presence of 60 μM citrate or 500 μM oxalate. It is known that both citrate anions and oxalate anions form complexes with iron as Fe(III)–citrate complex and Fe(III)–oxalate complex, respectively, which are more photoreactive for producing hydroxyl radicals under irradiation with visible light [23]. Also, it has been reported that iron oxide in clay minerals could dissolve more easily in the

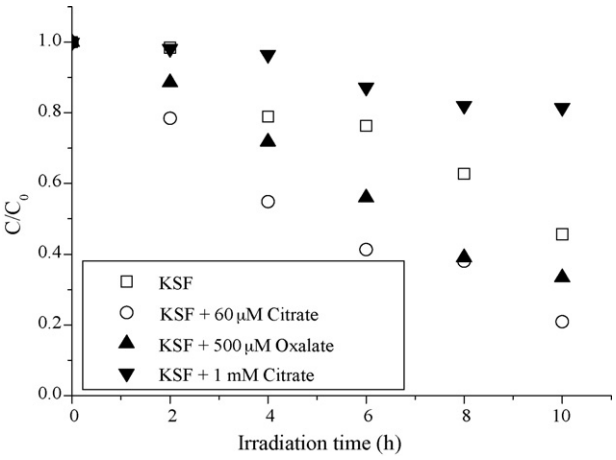

Fig. 8. Influence of carboxylic salts on the photodegradation of chloroform in aqueous solutions containing KSF. The experimental conditions were as follows: KSF 2.0 g L^{-1}, chloroform 0.42 mM, [citrate] = 60 μM and 1 mM, [oxalate] = 500 μM, irradiation time 10 h, pH 3.8.

presence of carboxylates under irradiation [25,26]. So, the degradation efficiency of chloroform was enhanced when greater amounts of photoactive iron ions were present in the KSF suspensions. The mechanism of formation of •OH by Fe(III)–carboxylate complex photolyzed and the structure iron dissolved were as followed (Eqs. (12)–(17)):

$$Fe^{3+} - L \xrightarrow{h\upsilon} Fe^{2+} + L^{\bullet} \tag{12}$$

$$L^{\bullet} + O_2 \rightarrow O_2{}^{-\bullet} + \text{otherphotoproducts} \tag{13}$$

$$Fe^{2+} + O_2{}^{-\bullet} + H^+ \rightarrow Fe^{3+} + H_2O_2 \tag{14}$$

$$Fe^{2+} + H_2O_2 \rightarrow Fe^{3+} + {}^{\bullet}OH + OH^- \tag{15}$$

$$> Fe(III) + L \rightarrow > Fe(III)L \tag{16}$$

$$> Fe(III)L \xrightarrow{h\upsilon} Fe_2 + L' \tag{17}$$

(Fe^{3+}–L represents Fe(III)–carboxylate complex, > represents surface complex, $L^{\bullet}$ and L′ represent carboxylate radical and its oxidized product respectively).

Fig. 8 also showed that high concentrations of citrate (1 mM) inhibited chloroform photodegradation. Based on the above discussion, more •OH was produced by adding carboxylic anions into the system, which results in greater removal efficiency of chloroform. On the other hand, carboxylic anions also act as scavengers of hydroxyl radicals and hence compete with chloroform for •OH reactivity. So when the concentration of carboxylic anions is high enough (of the order of 1 mM), the photodegradation rate of chloroform is inhibited.

3.6. Effect of HA

Humic acids are natural organic polyelectrolytes that make up the greatest proportion of naturally occurring dissolved organic matter in aquatic environments and soils [27] and carry a huge variety of functional groups, the majority of which are carboxylic groups and phenolic hydroxy groups. They can either accelerate [28] or inhibit [29] the photodegradation process of organic contaminants in aqueous solutions. HA is often closely associated with clay minerals due to the strong complexation between surface metals and acidic organic ligands [30]. It is necessary, therefore, to investigate the KSF photocatalytic efficiency of chloroform degradation in the presence of HA.

As shown in Fig. 9, after 10 h illumination, the loss of chloroform was 18%, 64% and 71% in the KSF suspensions in the present

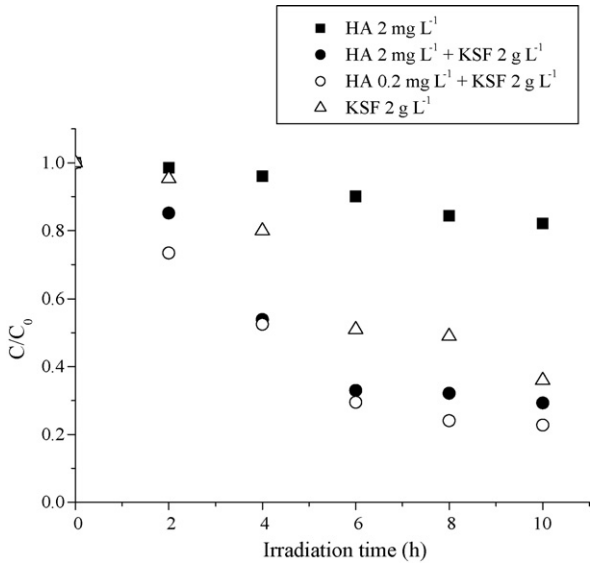

Fig. 9. Influence of HA on the photodegradation of chloroform in aqueous solutions containing KSF. The experimental conditions were as follows: KSF 2.0 g L^{-1}, chloroform 0.42 mM, irradiation time 10 h, pH 3.8.

of 2 mg L^{-1} HA, 2 g L^{-1} KSF, and both 2 mg L^{-1} HA and 2 g L^{-1} KSF respectively. This demonstrates that KSF with HA was better for the removal of chloroform than the individual action of KSF or HA. But when chloroform degradation rates with HA concentration of 0, 0.2 and 2 mg L^{-1} respectively were compared in the presence of KSF, the best chloroform degradation efficiency was achieved at an HA concentration of 0.2 mg L^{-1}. The HA and KSF system is complex. HA may form very stable complexes with iron in the KSF suspensions that could efficiently generate hydroxyl radicals through the mechanism of the photo-Fenton and Haber–Weiss reactions [31]. Furthermore, it has been reported that HA could adsorb onto the mineral by van der Waals' forces, hydrogen bonding, and cation exchange [32]. It is believed that the surface HA-clay complexation reactions affect the transport and transformation of substances in environmental systems [33]. However, in the case of HA and KSF suspensions, KSF cooperating with the appropriate concentration of HA could accelerate the degradation of chloroform. Nevertheless, further studies are needed to clarify to how HA affects the photodegradation of chloroform by KSF.

4. Conclusions

Under a black light lamp ($\lambda = 365$ nm), the photodegradation of chloroform in aqueous solutions catalyzed by KSF takes place via oxidation with •OH photogenerated mainly from the iron species in KSF. The degradation kinetics of chloroform follows the Langmuir–Hinshelwood rate law. The photodegradation rate of chloroform increased with increased concentrations of KSF in aqueous solutions in the range of 0–4.0 g L^{-1}; at higher concentrations of the order of 6.0 and 10.0 g L^{-1} KSF, the chloroform degradation efficiency decreased. The photodegradation of chloroform catalyzed by KSF was strongly pH-dependent. An increase of pH was accompanied by a decrease of the chloroform degradation efficiency. This pH effect is perfectly linked with the concentration of soluble iron that increases at more acidic pH levels. In addition, the removal efficiency of chloroform can be enhanced in the presence of carboxylic acid, but the concentrations of carboxylates should be controlled since excessive quantities of carboxylic salts compete with chloroform for •OH reactivity. Furthermore, the addition of low concentrations of HA in the KSF suspensions could enhance the photodegradation of chloroform. Thus all these results show that KSF could be considered as a new and efficient photocatalyst and as an alternative way for wastewater treatment. Its concentration, solution pH and presence of iron complexing agents must be taken into account as major parameters to improve the efficiency of such a process.

Acknowledgements

This research was supported by the National Natural Science Foundation of P.R. China (No. 40503016).

References

[1] M.E. Meek, R. Beauchamp, G. Long, D. Moir, L. Turner, M. Walker, Chloroform: exposure estimation, hazard characterization, and exposure-response analysis, J. Toxicol. Environ. Health Part B 5 (2002) 283–334.
[2] B. Mounir, M.N. Pons, O. Zahraa, A. Yaacoubi, A. Benhammou, Discoloration of a red cationic dye by supported TiO_2 photocatalysis, J. Hazard. Mater. 148 (2007) 513–520.
[3] P. Lu, F. Wu, N.S. Deng, Enhancement of TiO_2 photocatalytic redox ability by β-cyclodextrin in suspended solutions, Appl. Catal. B 53 (2004) 87–93.
[4] M.M. Cheng, W.H. Ma, C.C. Chen, J.N. Yao, J.C. Zhao, Photocatalytic degradation of organic pollutants catalyzed by layered iron(II) bipyridine complex–clay hybrid under visible irradiation, Appl. Catal. B 65 (2006) 217–226.
[5] J.H. Ramirez, C.A. Costa, L.M. Madeira, G. Mata, M.A. Vicente, M.L. Rojas-Cervantes, A.J. López-Peinado, R.M. Martín-Aranda, Fenton-like oxidation of Orange II solutions using heterogeneous catalysts based on saponite clay, Appl. Catal. B 71 (2007) 44–56.
[6] W.J. Song, M.M. Cheng, J.H. Ma, W.H. Ma, C.C. Chen, J.C. Zhao, Decomposition of hydrogen peroxide driven by photochemical cycling of iron species in clay, Environ. Sci. Technol. 40 (2006) 4782–4787.
[7] Z.G. Xiong, Y.M. Xu, L.Z. Zhu, J.C. Zhao, Enhanced photodegradation of 2,4,6-trichlorophenol over palladium phthalocyaninesulfonate modified organobentonite, Langmuir 21 (2005) 10602–10607.
[8] T. Katagi, Photodegradation of esfenvalerate in clay suspensions, J. Agric. Food Chem. 41 (1993) 2178–2183.
[9] B. Subramanian, G. Gupta, Adsorption of trace elements from poultry litter by montmorillonite clay, J. Hazard. Mater. 128 (2006) 80–83.
[10] P.P. Selvam, S. Preethi, P. Basakaralingam, N. Thinakaran, A. Sivasamy, S. Sivanesan, Removal of rhodamine B from aqueous solution by adsorption onto sodium montmorillonite, J. Hazard. Mater. 155 (2008) 39–44.
[11] W. Kwan, B.M. Volker, Rates of hydroxyl radical generation and organic compound oxidation in mineral-catalyzed Fenton-like systems, Environ. Sci. Technol. 37 (2003) 1150–1158.
[12] D. Habibi, O. Marvi, Montmorillonite KSF clay as an efficient catalyst for the synthesis of 1,4-dioxo-3,4-dihydrophthalazine-2(1*H*)-carboxamides and -carbothioamides under solvent-free conditions using microwave irradiation, Catal. Commun. 8 (2007) 127–130.
[13] C.A. Bowe, N. Krikorian, D.F. Martin, Extraction of heavy metals using modified montmorillonite KSF, Fla. Sci. 67 (2004) 74–79.
[14] H. Tamura, K. Goto, T. Yotsuyanagi, M. Nagayama, Spectrophotometric determination of iron(II) with 1,10-phenanthroline in the presence of large amounts of iron(III), Talanta 21 (1974) 314–318.
[15] X.L. Liu, F. Wu, N.S. Deng, Photoproduction of hydroxyl radicals in aqueous solution with algae under high-pressure mercury lamp, Environ. Sci. Technol. 38 (2004) 296–299.
[16] C. Feiyan, S.O. Pehkonen, M.B. Ray, Kinetics and mechanisms of UV-photodegradation of chlorinated organics in the gas phase, Water Res. 36 (2002) 4203–4214.
[17] A.L. Pruden, D.F. Ollis, Degradation of chloroform by photoassisted heterogeneous catalysis in dilute aqueous suspensions of titanium dioxide, Environ. Sci. Technol. 17 (1983) 628–631.
[18] C. Kormann, D.W. Bahnemann, M.R. Hoffmann, Photolysis of chloroform and other organic molecules in aqueous titanium dioxide suspensions, Environ. Sci. Technol. 25 (1991) 494–500.
[19] W. Choi, M.R. Hoffmann, Novel photocatalytic mechanisms for $CHCl_3$, $CHBr_3$, and $CCl_3CO_2^-$ degradation and the fate of photogenerated trihalomethyl radicals on TiO_2, Environ. Sci. Technol. 31 (1997) 89–95.
[20] C.-H. Chiou, R.-S. Juang, Photocatalytic degradation of phenol in aqueous solutions by Pr-doped TiO_2 nanoparticles, J. Hazard. Mater. 149 (2007) 1–7.
[21] G. Jozefaciuk, G. Bowanko, Effect of acid and alkali treatments on surface areas and adsorption energies of selected minerals, Clays Clay Miner. 50 (2002) 771–783.
[22] J.W. Stucki, K. Lee, L.Z. Zhang, R.A. Larson, Effects of iron oxidation state on the surface and structural properties of smectites, Pure Appl. Chem. 74 (2002) 2145–2158.
[23] F. Wu, N.S. Deng, Photochemistry of hydrolytic iron (III) species and photoinduced degradation of organic compounds. A minireview, Chemosphere 41 (2000) 1137–1147.
[24] P. Calza, C. Minero, E. Pelizzetti, Photocatalytic transformations of chlorinated methanes in the presence of electron and hole scavengers, J. Chem. Soc. Faraday Trans. 93 (1997) 3765–3771.

[25] M.C. Goldberg, K.M. Cunningham, E.R. Weiner, Aquatic photolysis: photolytic redox reactions between geothite and adsorbed organic acids in aqueous solutions, J. Photochem. Photobiol. A 73 (1993) 105–120.
[26] T.D. Waite, F.M.M. Morel, Photoreductive dissolution of colloidal iron oxide: effect of citrate, J. Colloid Interface Sci. 102 (1984) 121–137.
[27] J. Buffle, The analytical challenge posed by fulvic and humic compounds, Anal. Chim. Acta 232 (1990) 1–2.
[28] K. Hustert, P.N. Moza, A. Kettrp, Photochemical degradation of carboxin and oxycarboxin in the presence of humic substance and soil, Chemosphere 38 (1999) 3423–3429.
[29] J. Bachman, H. Patterson, Photodecomposition of the carbamate pesticide carbofuran: kinetics and the influence of dissolved organic matter, Environ. Sci. Technol. 33 (1999) 874–884.
[30] K. Kaiser, G. Guggenberger, The role of DOM sorption to mineral surfaces in the preservation of organic matter in soils, Org. Geochem. 31 (2000) 711–725.
[31] M. Paciolla, G. Davies, S. Jansen, Generation of hydroxyl radicals from metal-loaded humic acids, Environ. Sci. Technol. 33 (1999) 1814–1818.
[32] T.S. Arnarson, R.G. Keil, Mechanisms of pore water organic matter adsorption to montmorillonite, Mar. Chem. 71 (2000) 309–320.
[33] C. Koretsky, The significance of surface complexation reactions in hydrologic systems: a geochemist's perspective, J. Hydrol. 230 (2000) 127–171.